Clays and Clay Minerals, Vol. 44, No. 6, 811–817, 1996.

X-RAY DIFFRACTION ANALYSIS OF THIN CLAY FILMS FROM DILUTE SUSPENSIONS USING GLANCING INCIDENCE DIFFRACTION

KATHERINE OZALAS[1] AND BENJAMIN F. HAJEK[2]

[1] Eagan McAllister Associates, 2050 Mabelline Rd. Suite J, North Charleston, South Carolina 29406

[2] Department of Agronomy and Soils, Auburn University, Auburn, Alabama 36849

Abstract—X-ray diffraction (XRD) analysis of small quantities of clay mounted on glass slides using conventional Bragg-Brentano geometry generally produces unsatisfactory low-intensity reflections masked by amorphous substrate scatter. Glancing-incidence asymmetric Bragg diffraction, an alternative uncoupled geometry, uses a fixed low-incidence angle and parallel-beam optics to increase path length through the sample and decrease X-ray penetration into the substrate. To evaluate this technique on thin soil clay films, results from conventional Bragg-Brentano and glancing-incidence diffraction (GID) were compared for progressively diluted clay suspensions separated from 2 southeastern soils with typical mineral assemblages. Patterns produced by GID showed overall higher reflection intensities and reduced substrate scatter, especially at higher 2θ angles within the amorphous glass region. Using GID, positive identification of clay minerals was obtained from sample quantities as small as 0.005 mg cm^{-2} and suspensions as dilute as 29 mg L^{-1}.

Key Words—GID, Thin Films, XRD.

INTRODUCTION

The easiest, quickest, and probably most commonly used method of preparing oriented clay mounts for XRD is drying dilute suspensions of clay on a glass slide. In some instances, this may be the only feasible method due to sample size, characteristics or sampling method limitations. Although clay films prepared by this technique are well-oriented, they are often too thin to provide diffraction patterns with accurate relative intensities using a conventional diffractometer with Bragg-Brentano parafocusing geometry (Reynolds 1980). Problems associated with thin clay films on glass slides are especially accentuated at higher incidence angles, where deeper X-ray penetration results in a pattern dominated by amorphous glass slide scatter masking sample peaks.

Glancing-incidence asymmetric Bragg diffraction provides an alternative diffraction geometry for thin films without X-ray penetration depth problems associated with conventional Bragg-Brentano parafocusing geometry. GID is a non-focusing, parallel-beam geometry that allows a fixed low X-ray incidence angle (as low as 1° or less) throughout an uncoupled detector scan. Maintaining a low-incidence angle throughout the scan increases path length through the sample and decreases X-ray penetration depth, resulting overall in diffraction patterns with higher relative sample peak intensities and lower substrate scatter.

GID is an established procedure in both the electronics and materials science industries. Most commonly, GID is used for nondestructive characterization of the crystalline surface phase and physical structure of thin, epitaxially deposited films associated with magnetic tapes and superconductive and semiconductive materials (Huang et al. 1989; Toney and Brennan 1989; Pietsch et al. 1993; Rhan et al. 1993). GID has also been used to characterize surface textures and corrosion features of metals (Inyegar et al. 1987; Larsen et al. 1989; Szpunar et al. 1993). Although most GID thin-films studies have been conducted on specially designed diffractometers and/or with synchrotron radiation (Huang and Toney 1987; Lim et al. 1987; Cernik et al. 1990; Cui et al. 1991), some investigators have produced similar results employing a GID-modifying attachment on a standard diffractometer capable of independent θ/2θ measurement (Inyegar et al. 1987; Larsen et al. 1989; Huang 1990). For example, Larsen et al. (1989) measured a 50-Å film of Cr on a Si wafer, and Huang (1990) measured a 90-Å film of Fe_2O_3 on Fe_3O_4.

Previously studied thin-film materials like those mentioned above have crystallographic properties quite unlike clays, and one might expect significant differences from GID of thin clay films. In general, electronic-type thin films contain discrete layers of well-ordered, unmixed, single-phase compositions that produce sharp diffraction peaks. Many clays produce broad, diffuse, and poorly resolved diffraction peaks due to small particle size, a poorly ordered nature and/or interstratification. In addition, previously studied thin-film materials largely contain high-density metals with much higher linear absorption coefficients than clays. Because X-rays pass more readily through clays, larger sample quantities (that is, thicker films) might be required to produce a diffraction pattern. We are not aware of any study in which GID has been used on

Copyright © 1996, The Clay Minerals Society

https://doi.org/10.1346/CCMN.1996.0440612 Published online by Cambridge University Press

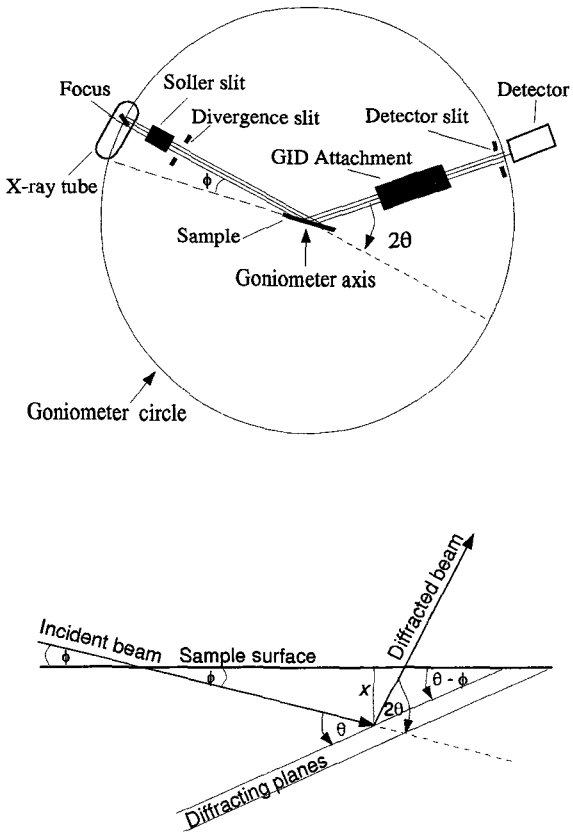


Figure 1. X-ray diffraction geometry for glancing incidence asymmetric diffraction (1a) and path of a diffracted X-ray beam in GID (1b).

clays; consequently its applicability to these minerals is essentially unknown.

This study was conducted to test the use of GID as a routine reconnaissance mineral-analysis technique for small sample quantities of clay (that is, thin clay films from dilute suspensions) and to compare GID results with conventional Bragg-Brentano XRD. In keeping with the goal of a routine reconnaissance technique, glass-slide suspension mounts were chosen for their widespread use and easy preparation. In addition, GID geometry was achieved through an easily removable attachment to a standard Siemens D5000 diffractometer, and conventional Bragg-Brentano XRD was conducted with the same instrument.

METHODS

Glancing-Incidence Asymmetric Bragg Diffraction and Parallel Beam Optics

In glancing-incidence asymmetric Bragg diffraction, the sample surface and X-ray source are set at a low-incidence angle and they remain stationary throughout the detector scan (Figure 1a). As first prescribed by Marra et al. (1979), GID makes use of total external reflection of X-rays incident at or below a critical angle, ϕ_c. At these low angles [typical ϕ_c values for diffracting materials are 0.2° to 0.6° for λ = 1.54 Å (Huang 1990)], X-rays are evanescent within the sample and penetrate only 100 Å or less. This technique is ideal for ultrathin films and surface phenomena studies, but, due to a severe loss of intensity and increased air scatter, synchrotron radiation is now often used for very low-angle scans. Later GID studies included incidence angles above the critical angle, yet still relatively low (ϕ = 1° to 2°). In this range, X-rays rapidly approach normal absorption behavior ($D = \sin \phi/\mu$), where μ = the linear absorption coefficient and D = the depth of penetration of X-rays. With these angles, X-ray penetration depth is effectively reduced to hundreds of thousands of Å by increasing the path length through the sample.

Because the glancing-incidence angle is fixed, the sample is scanned by moving the detector only and, unlike Bragg-Brentano geometry, a focusing circle is not maintained (Figure 1a). GID is a non-focusing geometric arrangement which makes use of parallel, rather than divergent, X-rays diffracted from suitably oriented crystallographic planes. An attachment placed between the diffracting planes and detector slit absorbs converging and diverging diffracted X-rays and allows only parallel X-rays to pass (Figure 1a) (Larsen et al. 1989). For the Siemens D5000, this attachment consists of a set of long, thin, parallel, horizontal, closely-spaced Soller slits made of a highly absorbing metal, Mo.

Sample Thickness Requirements

In order for XRD to provide a good analysis of clay films, samples must be thick enough to ensure that a significant proportion of the diffracted X-ray intensity is contributed by the sample, rather than by the underlying mount, at all $\theta/2\theta$ angles. This is not only necessary for achieving representative sample peak intensities for quantitative analysis, but is also qualitatively important for insuring that critical sample reflections are not missed.

In Bragg-Brentano geometry, the fraction of total diffracted intensity, G_x, contributed by a sample layer of thickness x is:

$$G_x = 1 - e^{-\mu 2x/\sin\theta} \quad [1]$$

where the X-ray path length for an incident angle θ is $2x/\sin\theta$ (Cullity 1967). If a sample has a sufficient thickness, x, then the X-ray path length through the sample is sufficient for essentially all X-rays to be absorbed or diffracted before they reach the mounting medium (G_x approaches 1). This thickness is known as "infinite thickness" and varies for a given diffracting material, depending upon its linear absorption coefficient and according to a particular $\theta/2\theta$ angle. Infinite thickness for most clays at 30 °2θ using Bragg-

https://doi.org/10.1346/CCMN.1996.0440612 Published online by Cambridge University Press

Table 1. Soil classification and % mineral composition of clay fraction (Angui 1991).

Soil	Classification	% Mineral composition				
		Gibbsite	Kaolinite	Verm./ smectite	Mica	Quartz
Benndale	Coarse-loamy, siliceous, thermic Typic Paleudults	8	35	39	7	0
Decatur	Clayey, kaolinitic, thermic Typic Hapludults	0	46	34	12	4

Brentano geometry is reached at 13–20 mg cm^{-2} of clay, depending on the specific clay minerals present (Bradley 1964; Rich 1975). If a clay film is less than infinite thickness, a proportion of X-ray beam intensity reaches the substrate, and sample reflections, especially those at higher θ/2θ angles where a greater thickness is required, may be undetected due to small sample quantity or masking by substrate scatter.

X-ray path length and the fraction of diffracted intensity for a given sample thickness with GID can be calculated with the same geometric relationships as Bragg-Brentano diffraction. In GID, X-rays are diffracted from planes lying at an angle, θ-ϕ, to the sample surface (Figure 1b), rather than parallel to the surface as in Bragg-Brentano geometry. The path length, l, for an incident angle ϕ and a Bragg angle 2θ and a sample thickness x is:

$$l = x\{(1/\sin \phi) + (1/\sin 2\theta\text{-}\phi)\} \quad [2]$$

The fraction of total diffracted intensity, G_x, diffracted by that thickness for GID geometry is:

$$G_x = 1 - e^{-\mu x\{(1/\sin \phi) + (1/\sin 2\theta\text{-}\phi)\}} \quad [3]$$

Equipment Setup

A Siemens D5000 diffractometer with a Cu target and a removable GID attachment was used for this study. Slit sizes and other diffractometer options (such as count times/step) for both geometries were chosen initially to resemble diffractometer setup for routine clay mineral analysis, although a diffracted beam crystal monochromator was used for all samples in Bragg-Brentano geometry only. The monochromator reduces the high, potentially peak-masking background associated with fluorescent X-rays from Fe (Moore and Reynolds 1989). A Siemens LiF monochromator designed for GID would likely produce more favorable results for this geometry; however, this hardware option was unavailable to us. In Bragg-Brentano geometry, a 1.0-mm divergent slit, a 1.0-mm detector slit and a 6.0-mm antiscatter slit were used. In GID, a Ni filter was used, and a divergent slit of 0.1 mm was used to reduce beam irradiation length due to very low incidence angles. All samples were initially run with a step size of 0.05° and a count time per step of 3 s on both geometries. Where weak reflections were observed using the standard setup (thinnest films), count time per step was increased to 20 s to enhance weak signals.

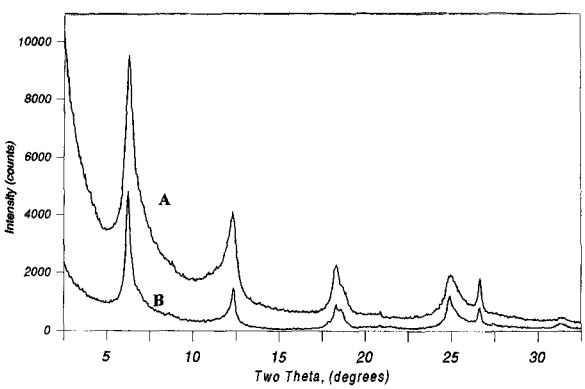


Figure 2. GID (A) and Bragg-Brentano XRD (B) analysis of a 12.5 mg cm^{-2} Benndale soil clay prepared on a glass slide.

Soil Samples

The soils chosen for study (Benndale and Decatur, both classified in the Ultisols order) represent typical clay mineral assemblages found in southeastern soils (Table 1). Standard procedures were used to remove organic matter and to separate and Mg-saturate clays prior to XRD analysis (Jackson 1956). A standard sample near infinite thickness (12.5 mg cm^{-2} of clay) for each soil clay was prepared by the patch transfer method (Drever 1973). Dilute suspensions of each soil clay containing 7.5 mg ml^{-1} were then made. For a sequence of more dilute suspensions (thinner films) of each soil clay, suspensions were successively diluted in half. Two ml of each suspension were dried on a 12-cm^2 glass slide at room temperature.

RESULTS

Major clay minerals observed in routine Bragg-Brentano XRD analysis of a Benndale and a Decatur sample are presented in Figures 2 and 3, respectively. Both samples contain a near infinite thickness at 30 °2θ, corresponding to 12.5 mg cm^{-2} of clay on a glass slide. Results from a ϕ = 1° GID analysis on these samples (Figures 2 and 3) show the same clay mineral assemblages with slightly different relative peak intensities. Overall, GID with a Ni filter produces higher

https://doi.org/10.1346/CCMN.1996.0440612 Published online by Cambridge University Press

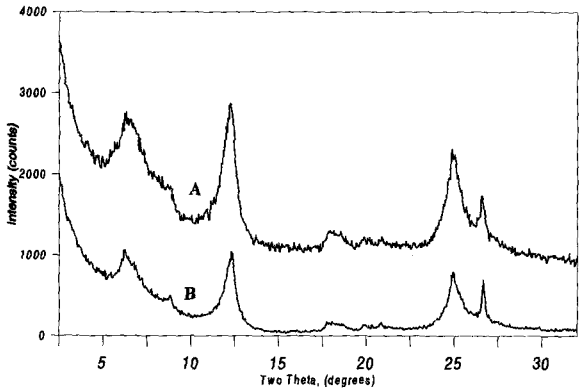


Figure 3. GID (A) and Bragg-Brentano XRD (B) analysis of a 12.5 mg cm^{-2} Decatur soil clay prepared on a glass slide.

peak intensities (nearly twice as intense for Benndale) and higher background.

GID and Bragg-Brentano XRD analysis of varying thicknesses of Benndale and Decatur films are shown in Figures 4 and 5, respectively. Peak intensities in GID are higher than Bragg-Brentano geometry for all thicknesses of both samples. Peak detection (signal-to-noise ratio) is also higher for most samples with GID, although the 10-Å peak is more readily detected in Bragg-Brentano geometry for several Decatur samples. Decatur clay films have more poorly detected sample reflections overall than Benndale films of the same quantities.

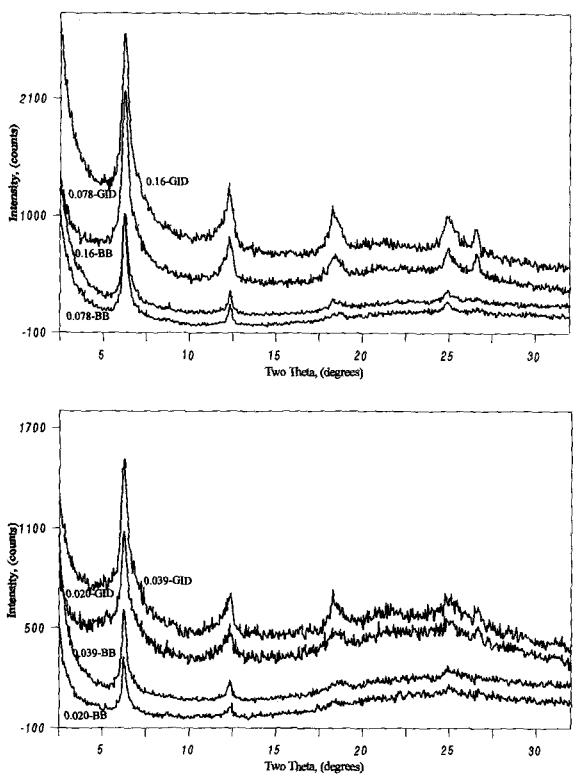


Figure 4. Benndale soil clay XRD patterns comparing sample quantities of 0.16 mg cm^{-2} (4a), 0.078 mg cm^{-2} (4a), 0.039 mg cm^{-2} (4b) and 0.020 mg cm^{-2} (4b) using GID (above in 4a and 4b) and Bragg-Brentano geometry (below in 4a and 4b).

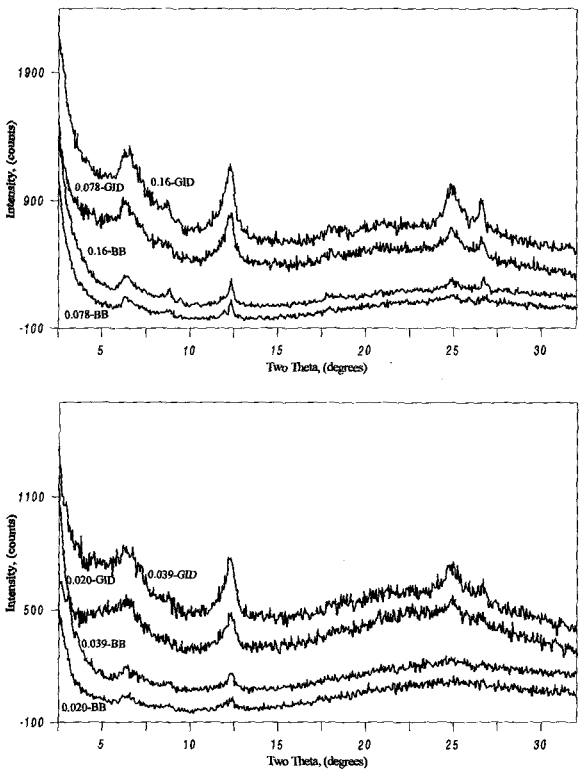


Figure 5. Decatur soil clay XRD patterns comparing sample quantities of 0.16 mg cm^{-2} (5a), 0.078 mg cm^{-2} (5a), 0.039 mg cm^{-2} (5b) and 0.020 mg cm^{-2} (5b) using GID (above in 5a and 5b) and Bragg-Brentano geometry (below in 5a and 5b).

As clay quantity (film thickness) decreases, a decrease in relative intensities of sample peaks is observed for both geometries. Initial loss of peaks in the high-angle range is observed in film with 0.078 mg cm^{-2} Bragg-Brentano geometry and the 0.020 mg cm^{-2} with GID for both soil clay compositions (Figures 4 and 5). Simultaneously, a significant intensity increase is observed in both geometries in the broad 20 to 30 °2θ peak due to amorphous scatter from the underlying glass slide. As the amount of clay decreases to 0.005 mg cm^{-2}, only a few weakly developed low-angle peaks are observed in either geometry (Figure 6).

The fraction of total diffracted intensity, G_x, for Benndale and Decatur clay quantities/cm^2 discussed above were calculated for both Bragg-Brentano, Equation [1], and GID, Equation [3], geometries (Figure 7).

https://doi.org/10.1346/CCMN.1996.0440612 Published online by Cambridge University Press

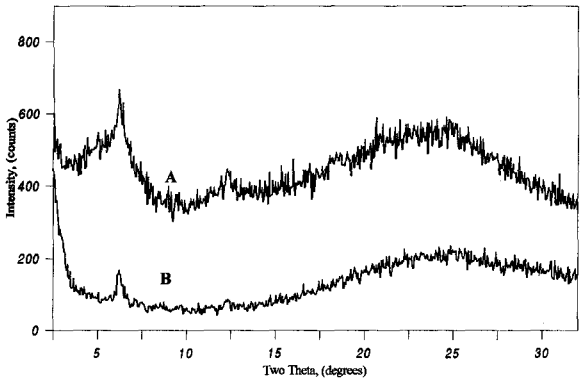


Figure 6. GID (A) and Bragg-Brentano XRD (B) of 0.005 mg cm^{-2} Benndale soil clay prepared on a glass slide.

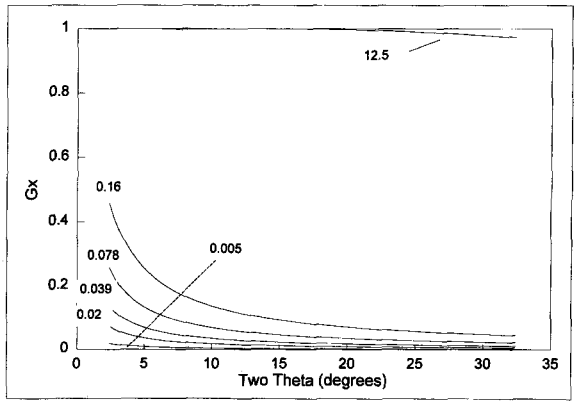
Both clay compositions were approximated to have a mass absorption coefficient:

$$\mu^* = \mu/\rho \qquad [4]$$

where μ = the linear absorption coefficient and ρ = density (Brindley 1961), of 40 mg cm^{-1} based on μ^* values of various clays reported in Carroll (1970). As expected, higher G_x were calculated for GID for a given clay quantity/area (film thickness), especially at higher 2θ values. For Bragg-Brentano geometry, curves for a given clay quantity (film thickness) show a rapid decline in G_x with higher 2θ angles. In contrast, curves are flat-lying for GID, reflecting diffracted intensity fractions controlled dominantly by clay film thickness. For these soil clays, sample peaks at higher 2θ angles (2θ > 15°) are detected for clay quantities (film thicknesses) with calculated $G_x > 0.08$. This relationship seems to be true for both GID (Figure 7a) and Bragg-Brentano (Figure 7b) geometries. Lower 2θ peaks, which have higher relative peak intensities overall at infinite thickness, are detected at even lower G_x values.

With smaller clay quantities (thinner films), improved detection and/or peak-to-noise ratio of clay reflections was achieved using GID by lowering the glancing angle and/or increasing count time per step. Decreasing the incidence angle from $\phi = 1°$ on 0.010 mg cm^{-2} Benndale sample, where only the broad amorphous peak is observed at higher 2θ values, to progressively lower incidence angles allowed detection of additional sample peaks. It also decreased glass scatter in the 20 to 30 °2θ range (Figure 8). An overall increase in relative intensities of lower 2θ angle peaks was also observed with a lower glancing angle (Figure 8). Increasing count time per step on the 0.005 mg cm^{-2} Benndale, $\phi = 0.6°$, from 3 s/step to 20 s/step further improved the signal-to-noise ratio of sample reflections using GID (Figure 9A).

Using Bragg-Brentano XRD on these same small-quantity clay samples (thin films), it was not possible



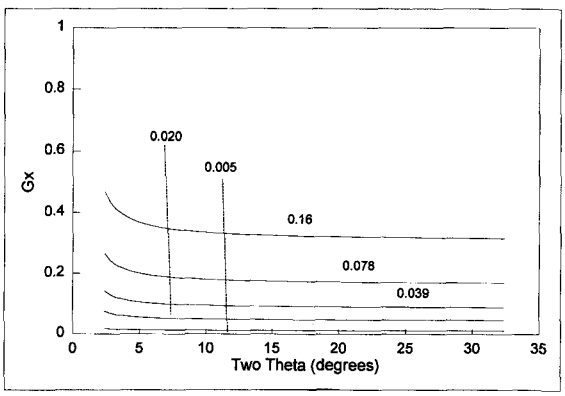


Figure 7. Calculated diffracted intensity fractions from soil clay films of approximate Benndale/Decatur composition and varying thicknesses with Bragg-Brentano (7a) and GID (7b) analysis.

to achieve comparable results to GID in peak detection and/or signal-to-noise ratio. Due to the focusing geometry of Bragg-Brentano XRD, a coupled scan is necessary, and the incidence angle cannot be independently set at a low angle to increase path length, as in

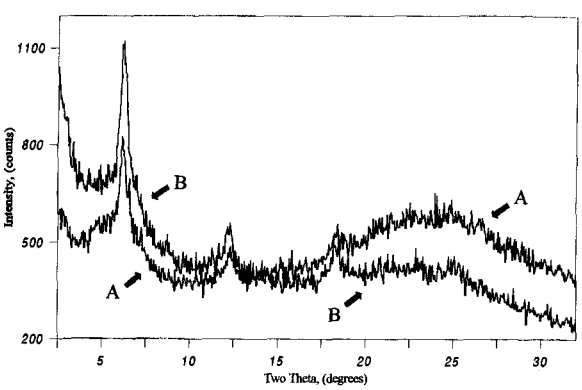


Figure 8. Increasing detection of clay peaks with decreasing glancing angle from 1.0° (A) to 0.6° (B) in GID analysis of a 0.010 mg cm^{-2} Benndale sample.

https://doi.org/10.1346/CCMN.1996.0440612 Published online by Cambridge University Press

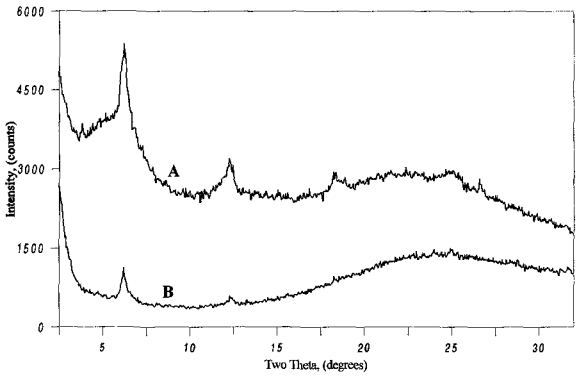


Figure 9. Increased signal-to-noise ratio of clay reflections of a 0.005 mg cm^{-2} Benndale sample with an increased count time/step from of 20 s (A) in GID compared with the same sample and count time/step in Bragg-Brentano geometry (B).

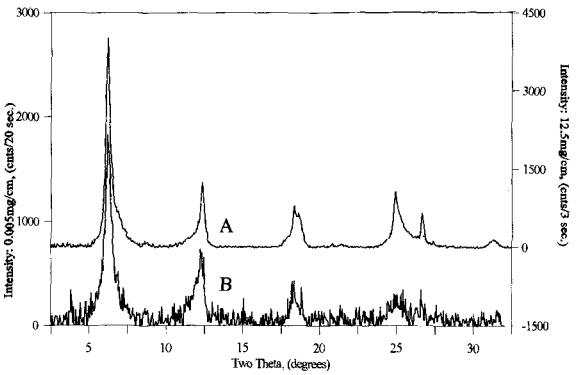


Figure 10. Comparison of GID of a 0.005 mg cm^{-2} Benndale soil clay (A) with Bragg-Brentano XRD of a near-infinite thickness, 12.5 mg cm^{-2}, of Benndale soil clay (B). Background has been subtracted in both geometries.

GID. Count time per step was increased for Bragg-Brentano XRD on the 0.005 mg cm^{-2} Benndale sample from 3 s/step to 20 s/step, as it was for GID, but the peak-to-noise ratio was not greatly improved as for GID (Figure 9B). Low-background single-crystal quartz sample substrates are widely used in mineral XRD analysis for small-quantity samples, and a 0.005 mg cm^{-2} Benndale clay film was dried onto a zero-background quartz slide and run in Bragg-Brentano geometry. For this thin clay film, the quartz substrate eliminated glass scatter but did not improve peak detection.

DISCUSSION AND CONCLUSIONS

Results from this study suggest that GID is a promising alternative to conventional Bragg-Brentano XRD for routine qualitative mineral analysis of thin clay films and/or small quantities of clay. For Benndale and Decatur soil clay compositions, GID provides better sample peak detection than conventional Bragg-Brentano XRD for clay films with 0.078 mg cm^{-2} clay or less. Using GID, the same clay mineral peaks, in similar relative intensities, were detected for a Benndale soil clay 0.005 mg cm^{-2} as were detected using conventional Bragg-Brentano XRD on a Benndale soil clay near infinite thickness 12.5 mg cm^{-2} (Figure 10). For the Decatur soil clays, detection of most clay mineral peaks was achieved in GID for slightly thicker films.

Differences in sample peak detection between Benndale and Decatur soil clays are more likely attributed to differences in sample compositions than to GID geometry. With GID, clay mineral peaks can be detected in thinner films (from more dilute suspensions) of Benndale clay separates than Decatur clay separates. Because Benndale clay mineral peaks are also better detected in samples near infinite thickness using conventional Bragg-Brentano XRD, compositional factors (such as mineral characteristics and proportions and particle size) are most likely affecting the detection of sample peaks for clay minerals in both geometries. This suggests that thickness limitations for the detection of specific mineral reflections in GID is somewhat dependent upon the composition of a given clay film. This would include not only the mineral characteristics, but also the phase abundance.

Our current GID setup is most useful in the analysis of higher 2θ reflections, where a greater thickness is needed in Bragg-Brentano XRD to achieve a higher G_x, and from 20 to 30 °2θ for glass slide suspension mounts, due to underlying glass scatter. For some clay compositions and moderate film thicknesses, Bragg-Brentano XRD may provide better detection of very low angle peaks (2.5 to 12 °2θ) than GID (for example, the 10-Å peak in the 0.63 mg cm^{-2} Decatur film). Low-angle peaks could be masked by a high background at low 2θ angles in GID. The position and shape of this background suggest that it is an effect of scatter from the sample holder caused by incident-angle length exceeding sample length (Jenkins and Squires 1982; Jenkins 1989), although this does not agree with calculations of incident-beam length from common equations (Moore and Reynolds 1989). A number of other diffractometer parameters can cause spurious broad peaks in the low-angle range (Brown and Brindley 1980); this problem will need to be further addressed in later studies.

GID offers many of the same benefits as conventional Bragg-Brentano XRD for clay mineral analysis (such as ease of sample preparation and low cost), without the sample thickness and quantity limitations. GID of clay films from quantities greater than 0.05 mg cm^{-2} can also produce results as quickly as Bragg-Brentano XRD, although longer count times may be required for thinner clay films. In addition, the parallel-beam, non-focusing optics used in GID may offer simpler and more straightforward calculations for quantitative analysis due to the elimination/reduction

https://doi.org/10.1346/CCMN.1996.0440612 Published online by Cambridge University Press

of focusing aberrations from flat specimen and sample displacement errors (Larsen et al. 1989; Parrish and Hart 1990). Most importantly, GID offers an uncoupled scan which allows an incidence angle to be specified for any Bragg angle. Incidence angles near the critical angle may be required for very thin clay films from more dilute suspensions (less than 0.20 mg cm^{-2} for the clay compositions studied). At incidence angles $< 1.0°$, overall intensity is reduced and air scatter is increased; however, signal-to-noise ratios can be improved by increasing count time/step to 20 s/0.05° or more.

A comparison of GID and Bragg-Brentano XRD for routine reconnaissance clay-mineral analysis suggests that GID may be most useful in studies that require minimum preparation of small clay quantities. Some examples include studies of naturally occurring dilute clay suspensions like those from soil surface runoff, streams or pond water. These suspensions can be placed directly on glass slides and dried, and clays can be analyzed without additional preparation.

GID may also aid in routine reconnaissance mineral analysis for clays whose physical properties prevent preparation of infinite thickness samples. Samples referred to as "curlers" or "peelers" shrink on drying and separate from the mounting medium. It is difficult to produce good 00*l* diffraction patterns from these samples (Moore and Reynolds 1989). With GID, a very small quantity of sample can be used per mount surface area, promoting greater cohesion to the mounting surface.

REFERENCES

Angui P. 1991. Potassium fixation and structural characterization of 2:1 phyllosilicates in clays from representative soils of the southeastern United States [dissertation]. Auburn, AL: Auburn University. 221 p.

Bradley, WF. 1964. X-ray diffraction analysis of soil clays and structure of clay minerals. In: Rich CI, Kunze GW, editors. Soil clay mineralogy. p 113–124.

Brindley GW. 1961. Quantitative analysis of clay mixtures. In: Brown G, editor. The X-ray identification and crystal structures of clay minerals. London: Mineralogical Society. p 489–516.

Brown G, Brindley GW. 1980. X-ray diffraction procedures for clay mineral identification. In: Brown G, Brindley GW, editors. Crystal structures of clay minerals and X-ray identification. London: Mineralogical Society. p 305–360.

Carroll D. 1970. Clay minerals: a guide to their X-ray identification: special paper 126. Boulder, CO: The Geological Society of America. 80 p.

Cernik RJ, Clark SM, Pattison P. 1990. Study of thin films and multilayers using energy-dispersive diffraction of synchrotron radiation. Adv X-ray Anal 33:101–107.

Cui SF, Mai ZH, Wu LS, Wang CY, Dai DY. 1991. A new scheme for X-ray grazing incidence diffraction. Rev Sci Instrum 62:2419–2423.

Cullity BD. 1967. Elements of X-ray diffraction. Reading, MA: Addison-Wesley. 514 p.

Drever JI. 1973. The preparation of oriented clay mineral specimens for X-ray diffraction analysis by a filter-membrane peel technique. Am Mineral 58:553–554.

Huang TC. 1990. Surface and ultra-thin film characterization by grazing-incidence asymmetric Bragg diffraction. Adv X-ray Anal 33:91–99.

Huang TC, Segmuller A, Lee W, Lee V, Bullock D, Karimi R. 1989. X-ray diffraction analysis of high Tc superconducting thin films. Adv X-ray Anal 32:269–277.

Huang TC, Toney MF. 1987. Analysis of cobalt-doped iron oxide thin films by synchrotron radiation. Thin Solid Films 154:439–445.

Inyegar SS, Santana MW, Windischmann H, Engler P. 1987. Analysis of surface layers and thin films by low incident angle X-ray diffraction. Adv X-ray Anal 30:458–464.

Jackson ML. 1956. Soil chemical analysis—advanced course. Madison, WI: ML Jackson, Univ of Wisconsin. 894 p.

Jenkins R. 1989. Instrumentation. In: Bish DL, Post JE, editors. Modern powder diffraction. Reviews in Mineralogy 20. Washington, DC: Mineralogical Society of America. p 19–45.

Jenkins R, Squires B. 1982. Problems in the measurement of large d-spacings with the parafocusing diffractometer. Norelco Reporter 29:20–25.

Larsen RA, McNulty TF, Goehner RP, Crystal KR. 1989. X-ray diffraction studies of polycrystalline thin films using glancing angle diffractometry. Adv X-ray Anal 32:311–321.

Lim G, Parrish W, Masciochicci N. 1987. Grazing incidence synchrotron X-ray diffraction method for analyzing thin films. J Mater Res 2:471–477.

Marra WC, Eisenberger P, Cho AY. 1979. X-ray total external reflection—Bragg diffraction: A structural study of the GaAs-Al interface. J Appl Phys 50:6927–6933.

Moore DM, Reynolds RC. 1989. X-ray diffraction and the identification and analysis of clay minerals. New York: Oxford Univ Pr. 332 p.

Parrish W, Hart M. 1990. Parallel beam and focusing X-ray powder diffractometry. Adv X-ray Anal 32:481–488.

Pietsch U, Metzger H, Rugel S, Jenichen B, Robinson IK. 1993. Depth-resolved measurement of lattice relaxation in $Ga_{1-x}As/GaAs$ strained layer superlattices by means of grazing-incidence X-ray diffraction. J Appl Phys 74:2381–2387.

Reynolds RC. 1980. Interstratified clay minerals. In: Brown G, Brindley GW, editors. Crystal structures of clay minerals and their X-ray identification. Monograph No. 5. London: Mineralogical Society. p 249–303.

Rhan H, Pietsch U, Rugel S, Metzger H, Peisl J. 1993. Investigations of semiconductor superlattices by depth-sensitive X-ray methods. J Appl Phys 74:146–152.

Rich CI. 1975. Amount of clay needed for optimum X-ray diffraction analysis. Soil Sci Soc Am Proc 39:161–162.

Szpunar JA, Ahlroos S, Tavernier Ph. 1993. Method of measurement and analysis of texture in thin films. J Mater Sci 28:2366–2376.

Toney MF, Brennan S. 1989. Structural depth profiling of iron oxide thin films using grazing incidence asymmetric Bragg X-ray diffraction. J Appl Phys 65:4763–4768.

(Received 17 February 1995; accepted 26 February 1996; Ms. 2625)

https://doi.org/10.1346/CCMN.1996.0440612 Published online by Cambridge University Press